Activity-induced Internalization and Rapid Degradation of Sodium Channels in Cultured Fetal Neurons

Christophe Paillart,* Jean-Louis Boudier,* Jeanne-Andrée Boudier,* Hervé Rochat,‡ François Couraud,* and Bénédicte Dargent*

*Institut National de la Santé et de la Recherche Médicale Unité 374; and Centre National de la Recherche Scientifique URA 1455, Institut Jean Roche, Faculté de Médecine Secteur Nord, 13916 Marseille Cedex 20 France

Abstract. A regulatory mechanism for neuronal excitability consists in controlling sodium channel density at the plasma membrane. In cultured fetal neurons, activation of sodium channels by neurotoxins, e.g., veratridine and α-scorpion toxin (α-ScTx) that enhance the channel open state probability induced a rapid down-regulation of surface channels. Evidence that the initial step of activity-induced sodium channel down-regulation is mediated by internalization was provided by using ^{125}I-α-ScTx as both a channel probe and activator. After its binding to surface channels, the distribution of ^{125}I-α-ScTx into five subcellular compartments was quantitatively analyzed by EM autoradiography. ^{125}I-α-ScTx was found to accumulate in tubulovesicular endosomes and disappear from the cell surface in a time-dependent manner. This specific distribution was prevented by addition of tetrodotoxin (TTX), a channel blocker.

By using a photoreactive derivative to covalently label sodium channels at the surface of cultured neurons, we further demonstrated that they are degraded after veratridine-induced internalization. A time-dependent decrease in the amount of labeled sodium channel α subunit was observed after veratridine treatment. After 120 min of incubation, half of the α subunits were cleaved. This degradation was prevented totally by TTX addition and was accompanied by the appearance of an increasing amount of a 90-kD major proteolytic fragment that was already detected after 45–60 min of veratridine treatment. Exposure of the photoaffinity-labeled cells to amphotericin B, a sodium ionophore, gave similar results. In this case, degradation was prevented when Na^+ ions were substituted by choline ions and not blocked by TTX. After veratridine- or amphotericin B–induced internalization of sodium channels, breakdown of the labeled α subunit was inhibited by leupeptin, while internalization was almost unaffected. Thus, cultured fetal neurons are capable of adjusting sodium channel density by an activity-dependent endocytotic process that is triggered by Na^+ influx.

THE voltage-sensitive sodium channel, a plasma membrane glycoprotein, is an important determinant of neuronal excitability. The rat brain Na^+ channel consists of a major α subunit (260 kD), a noncovalently associated β_1 subunit (36 kD), and a disulfide-linked β_2 subunit (33 kD) (Hartshorne and Catterall, 1984; Isom et al., 1994). The expression of several genes encoding the α subunit is temporally and spatially regulated in the central nervous system and begins early in embryonic development (for review see Mandel, 1992; Noda et al., 1986, Beckh et al., 1989; Joho et al., 1990; Brysch, 1991; Gautron et al., 1992; Schaller et al., 1995). In contrast, the β_1 subunit is encoded by a unique gene in neurons as well as in other excitable tissues (Isom et al., 1992; Makita et al., 1994). The β_2 subunit contains a cell adhesion molecule motif in the extracellular NH_2-terminal domain and has the ability to expand cell membrane area when expressed in *Xenopus* oocytes (Isom et al., 1995*b*). Although the α subunit alone is sufficient to form voltage-sensitive and selective ion channels (Suzuki et al., 1988, Joho et al., 1990; Scheuer et al., 1990), its functional properties are modified by coexpression with the β_1 subunit (Isom et al., 1992, 1995*a*) or with the β_2 subunit (Isom et al., 1995*b*) in *Xenopus* oocytes and in mammalian cell lines.

Sodium channels are involved in the generation and conduction of action potentials along the plasma membrane. Thus, their specific distribution and density are two important factors that control neuronal excitability. One of the best examples is the myelinated axon, where the distribution of sodium channels is restricted to the node of Ranvier (Waxman and Ritchie, 1985). In retinal ganglion cells, a high density of sodium channels was detected by

Address correspondence to Bénédicte Dargent , INSERM U 374, Institut Jean Roche, Faculté de Médecine Secteur Nord, Boulevard Pierre Dramard, 13916 Marseille Cedex 20 France. Tel.: 33 91698954. Fax: 33 91090506.

1. *Abbreviations used in this paper*: AaHII, toxin II from *Androctonus australis* Hector; α-ScTx, α-scorpion toxin; LqqV, toxin V from *Leiurus quinquestriatus quinquestriatus*; $[Na^+]_i$, intracellular Na^+ concentration; STX, saxitoxin; TTX, tetrodotoxin.

immunocytochemistry at axon hillocks that may account for the low threshold for action potential initiation (Wollner and Catterall, 1986). However, their distribution is not restricted to this domain. Sodium channels are located in the soma (Boudier et al., 1985; Westenbroek et al., 1989), as well as in dendrites as demonstrated by imaging and by electrophysiological recording from hippocampal pyramidal cells (Jaffe et al., 1992; Spruston et al., 1995; Magee and Jonhston, 1995) and from neocortical pyramidal cells (Stuart and Sakmann, 1994). By generating retrograde spike conduction from soma to dendrites (Stuart and Sakmann, 1994; Spruston et al., 1995), sodium channels also play a role in subtle integrative processes.

The molecular mechanisms involved in the control of the localization and density of sodium channels are poorly understood. We have previously shown that channel number is regulated at the cell surface (Dargent and Couraud, 1990; Dargent et al., 1994). In cultured fetal neurons, the activation of sodium channels by agents that enhance the channel open state probability (e.g., veratridine and α-scorpion toxin [α-ScTx][1] induced a rapid ($t_{1/2}$ = 15 min) down-regulation of surface channels. The possibility that membrane depolarization mediates Na^+ channel down-regulation is unlikely because the density of sodium channel was not affected by increasing extracellular K^+ concentration (50 mM KCl) (Dargent and Couraud, 1990). Sodium channel down-regulation was not provoked by an increase in intracellular Ca^{2+} concentration induced either by a Ca^{2+} ionophore, A23187, or by a Ca^{2+}-ATPase blocker, thapsigargin (Dargent et al., 1995.). One of the particular features of sodium channel down-regulation is that it is not evoked by neurotoxin binding itself, but results from an increase in Na^+ influx through the activated channel. It is prevented by tetrodotoxin (TTX), a channel blocker, and by substitution of sodium ions by either choline (a nonpermeant ion) or Li^+ (a permeant ion). Furthermore, down-regulation can be induced by a sodium ionophore such as amphotericin B. This activity-dependent phenomenon is selective for sodium channels. No decrease in the surface density of other ion channels and receptors, i.e., apamin-sensitive K^+ channels, N-type Ca^{++} channels, and insulin receptors was observed. Thus, activity induced down-regulation may provide an important regulatory process allowing neurons to adjust sodium channel density at the cell surface and therefore control excitability.

Endocytosis of cell surface receptors and other membrane proteins is a process by which integral membrane proteins are selectively internalized from the plasma membrane (for review see Gruenberg and Maxfield, 1995). Endocytosed membrane proteins appear first in early endosomes and some of them are recycled back to the membrane while others are transported to late endosomes and lysosomes to be degraded. One of the questions raised by our findings is whether the initial step of activity-induced sodium channel down-regulation is mediated by internalization. By using ^{125}I-α-ScTx, as both a channel probe and activator, we showed previously (Dargent et al., 1994), that a fraction of the α-ScTx appears to be internalized because it was not released into the medium by an acid wash. In the present study, we have used ultrastructural methods and covalent labeling to monitor the intracellular fate of sodium channels.

In cultured fetal neurons, an EM autoradiography study was carried out to quantify the distribution of ^{125}I-α-ScTx in different subcellular structures after its binding to cell surface sodium channels. In a time-dependent manner, after induction of down-regulation, ^{125}I-α-ScTx was found to specifically accumulate in tubulovesicular endosomes. Furthermore, by using a photoaffinity labeling procedure to label surface sodium channels, we obtained evidence that, upon neurotoxin activation or amphotericin B treatment, channel α subunits are degraded in a leupeptin-sensitive compartment.

Materials and Methods

Materials

Toxin II from *Androctonus australis* Hector (AaHII) and toxin V from *Leiurus quinquestriatus quinquestriatus* (LqqV) were purified as described (Martin and Rochat, 1986). FCS was purchased from Boehringer-Mannheim Biochemicals (Mannheim, Germany), TTX from Latoxan (Rosans, France), veratridine and leupeptin from Sigma Chemical Co. (St. Louis, MO). Amphotericin B was from GIBCO BRL (Cergy-Pontoise, France). ANB-NOS (*N*-5-azido-2-nitrobenzoyloxy-succinimide) was from Pierce (Oud Beijerland, The Netherlands). [^{3}H]saxitoxin ([^{3}H]STX), (29–37 Ci/mmol) and carrier-free Na^{125}I were obtained from Amersham Corp. (Les Ulis, France).

Scorpion Toxin Derivatives

α-Scorpion toxins were radio labeled by lactoperoxydase-catalyzed iodination (Jover et al., 1988) and purified by immunoprecipitation (^{125}I-AaHII) or by batch-wise resuspension with Dowex 1-X8 ion exchanger (^{125}I-LqqV). ^{125}I-AaHII was used for EM autoradiography; however as this toxin loses its biological activity upon modification of the lysines, it was replaced by ^{125}I-LqqV for photolabeling experiments (Jover et al., 1988). A photoreactive derivative of ^{125}I-LqqV was prepared by incubation with ANB-NOS (De Lima et al., 1988) and used immediately after preparation.

Cell Culture

Fetal rat brain neurons were cultured as previously described (Dargent et al., 1994). Briefly, brains from 16-d-old Wistar rat embryos were mechanically dissociated and cultured in DME supplemented with 5% FCS and antibiotics. Cells were plated at a density of 10^6 per ml. [^{3}H]STX binding experiments were performed as previously described (Dargent et al., 1994).

Electron Microscopy and Autoradiography

Fetal rat brain neurons (d 11 in vitro) cultured in 12-well plates (Costar Corp., Cambridge, MA) were incubated with 2 nM ^{125}I-α-ScTx either in the presence or absence of 1 μM TTX for 20 or 60 min at 37°C. At the end of the incubation, cells were rapidly rinsed three times with 1 ml of precooled binding buffer (140 mM choline Cl, 5 mM KCl, 0.8 mM $MgSO_4$, 1.8 mM $CaCl_2$, 0.1% BSA, 20 mM Hepes, adjusted to pH 7.4 with Tris base) and once with phosphate buffer and were processed for EM: fixation in 2.5% glutaraldehyde solution in 0.13 M sodium phosphate buffer; postfixation in 2% OsO_4 solution; after long rinses, en bloc staining in 2% ethanolic uranyl acetate solution, and dehydration. Then, the culture was cut with the tip of a scalpel blade, and the small squares (~ 1 mm wide) detached from well using propylene oxyde (Griffiths et al., 1984). They were flat-embedded in Epon as multilayered stacks. Ultrathin vertical sections were collected on collodion-coated slides, and autoradiograms were prepared according to Larra and Droz (1970), using emulsion (L4; Ilford, St Priest, France) and Microdol X (Kodak, Paris, France) development after 56 d of exposure.

Quantitative Analysis

Three independent culture wells per experimental condition were used. For each well, three blocs were randomly chosen for ultrathin sectioning.

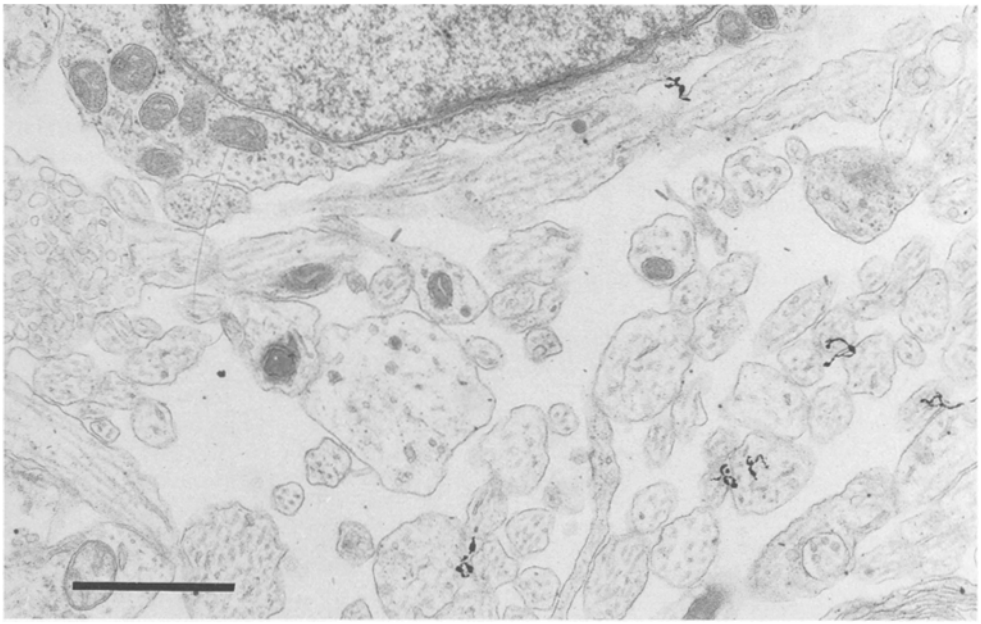

Figure 1. Fetal neurons culture. Randomly oriented processes, with apparent diameter varying between less than 0.2–2 μm, occupied most of the fields. Perikaryal profiles were less frequent, localized in the upper layer of the cell culture. Bar, 1 μm.

First, background and global signal to background ratio were assessed by the quadrat method (Williams, 1977). The background on section areas devoid of cell structures was very low, at maximum 0.3×10^{-3} grains per μm^2 of section surface; the signal to background ratio was in all cases satisfactory, higher than 35. Then, twelve micrographs per bloc (magnification × 11,500) were systematically sampled at each intersection of the culture layer with the supporting grid. Autoradiograms were analyzed by the "circle method" (Williams, 1977). This method uses circles to attribute the radioactivity to cell structures, including those without substantial section area. In pratice, a circle is centered on each actual silver grain, and grains are attributed to predefined "compartments" depending on structures appearing in the circle. The distribution of these "grains" (i.e., circles centered on actual silver grains) is compared with those of circles at the same size regularly distributed on micrographs (subsequently designated as "circles"), corresponding to an hypothetical randomly distributed grain set. Circle diameter was adjusted to give 50% probability of the radioactive source falling in the circle, 0.35 μm in the present study. The culture was divided into six primary compartments, that could be sampled individually. Sampling generated junctional and compound compartments (i.e., compartments where the circle fell on the frontier between two or three primary compartments), giving a final total of 19 compartments. An overlay printed with 56 regularly arranged circles was used to attribute circles to the defined compartments. The number of grains analyzed in each experimental condition ranged between 278 and 335, and the circle to grain ratio was ~20. After completing data collection, compartments with consistent biological interest were regrouped, if necessary, to obtain grain and normalized circle data greater than 5. Crude specific radioactivities (mean ± SD) were calculated according to Williams (1977).

Photoaffinity Labeling of Cultured Neurons with ^{125}I-ANB-LqqV

Neurons, cultured in 60-mm dishes (Costar Corp.), were quickly rinsed twice with sodium buffer containing of 140 mM NaCl, 5 mM KCl, 10 mM glucose, 0.8 mM $MgSO_4$, 1.6 mM $CaCl_2$, 0.1% BSA and 20 mM Hepes, adjusted to pH 7.4 with Tris base, at 37°C. Then, cells were incubated in sodium buffer containing 2 nM ^{125}I-ANB-LqqV and 1 μM of TTX for 30 min in the dark at 37°C, and then irradiated at 4°C, for 5 min at ~5 cm from a ventilated 125-w mercury vapor lamp (λ_{max} = 356 nm) (Philips Electronic Instruments Co., Mahwah, NJ). Bound TTX was released by washing the cells 3 times for 7 min each with sodium buffer at 37°C and internalization was initiated by adding 20 μM veratridine. In control cells, 1 μM of TTX was present during subsequent steps. The cells were rinsed three times with PBS, scraped in 0.32 M sucrose, 5 mM Tris buffer at pH 7.4 containing protease inhibitors (1 mM iodoacetamide, 0.8 mM pefabloc, 2 μM pepstatin A, and 1 mM EDTA), and homogenized. Nuclei were eliminated by centrifugation for 10 min at 800 *g* and membranes were collected at 100,000 *g* for 30 min.

SDS-PAGE and Autoradiography

Membrane samples were solubilized with 70 mM Tris, 10 mM EDTA, 6% sucrose, 3% SDS, and 10 mM β-mercaptoethanol at pH 9 and denaturated for 5 min at 100°C. Samples were then analyzed by SDS–gel electrophoresis on to 5–15% or 5–10% acrylamide gradient gels (Maizel, 1971), followed by autoradiography using Kodak-X-Omat film in cassettes with intensifying screens at −80°C or analysis using a PhosphorImager (Molecular Im-

Table I. Definitions of Compartments Used in the Circle Analysis

Number	Names	Definitions
1	Cytoplasm	Cytoplasm of soma and cell processes, including all intracytoplasmic structures except those of compartment 2.
2	Tubules-vesicles	Intracytoplasmic membrane structures, whatever their apparent shape, size, or content, either exclusively or associated with surrounding cytoplasm. Granular reticulum, clearly identifiable Golgi stack elements and nucleus were considered as parts of the compartment 1.
3	Cell membrane	Cell membrane, plus the associated cytoplasm and extracellular space included in the circle.
4	Shared tubulovesicular membrane	Cell membrane defined in 3, plus one structure defined in 2.
5	Extracellular	Extracellular space

ager GS-250; Bio-Rad Laboratories). Quantitation of radioactivity on the gels was performed with software (Molecular Analyst; Bio-Rad Laboratories).

Results

Time-dependent Localization of ^{125}I-α-ScTx in Vesicular-tubular Compartment upon its Binding to Surface Sodium Channels

α-ScTx binds specifically with high affinity to sodium channels and therefore is currently used as a marker to study channel distribution (Boudier et al., 1985, 1992). In cultured fetal neurons, α-ScTx, which causes channel activation by increasing the opening state probability, was shown to provoke rapid channel down-regulation (Dargent and Couraud, 1990). To demonstrate that the initial step of sodium channel down-regulation is mediated by internalization, we examined the distribution of ^{125}I-α-ScTx in different subcellular structures by quantitative EM autoradiography. Cultured neurons were incubated at 37°C

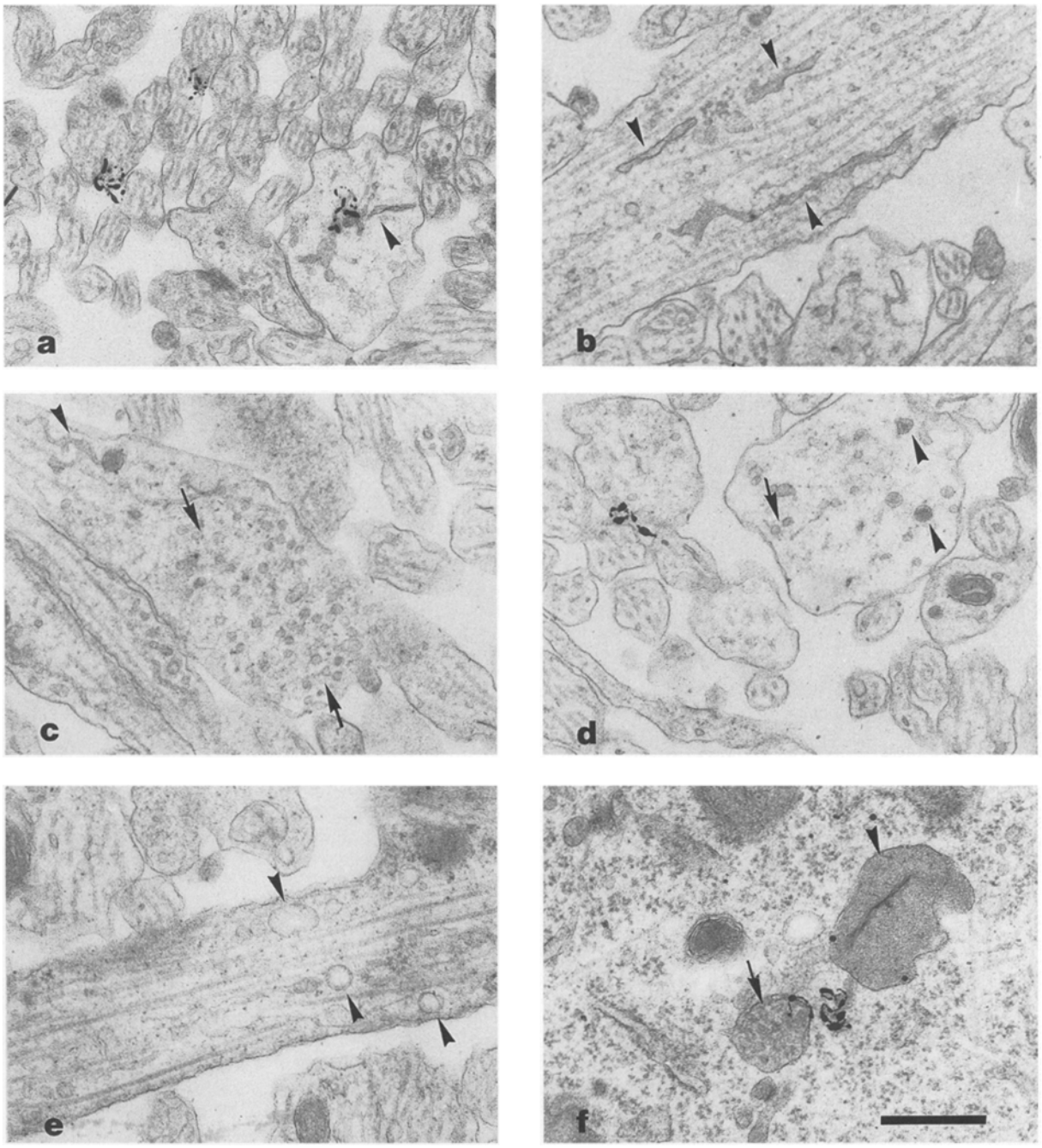

Figure 2. Examples of structures attributed to the tubulovesicular compartment. In the processes, structures attributed to the tubulovesicular compartment looked often as narrow tubules (*a* and *b*, *arrowheads*), sometimes branched (*c*, *arrowhead*) or vesicular in shape, similar in size to synaptic vesicles (*c* and *d*, *arrows*), less frequently with a dense core (*d*, *arrowheads*), or vacuolar with electron-lucent content (*e*, *arrowheads*). In the cell bodies (*f*), this compartment was mainly represented by large dense bodies (*arrowhead*), and also multivesicular bodies (*arrow*). Bar, 0.5 μm.

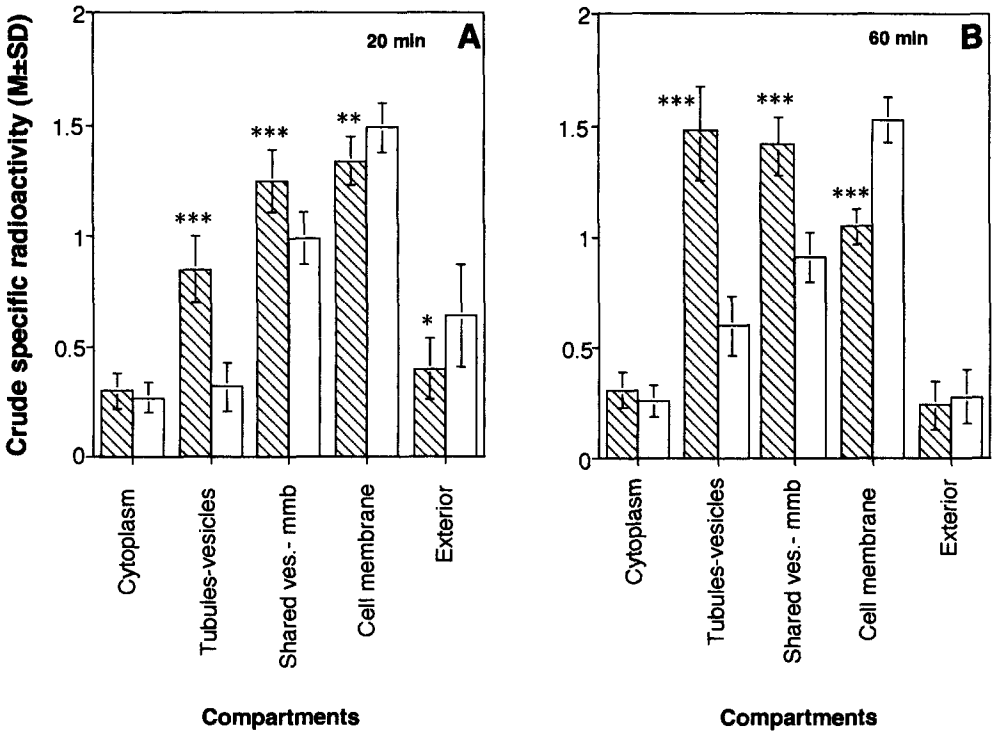

Figure 3. Distribution of radioactivity in cultured fetal neurons incubated with ^{125}I-α-ScTx. Cells were incubated at 37°C with 2 nM ^{125}I-α-ScTx either in the absence (activated cells) or in the presence of 1 μM TTX (control cells), for 20 min (*A*) or 60 min (*B*). After EM autoradiography, the radioactivity was quantitatively analyzed into five compartments defined in Table I. *Ves.-mmb*, vesicles-membrane. Results are expressed as mean ± SD. Asterisks indicate significant difference from activated with control cells. *t*-test: $*P < 0.05$, $**P < 0.01$, $***P < 0.001$. ▧, activated cells; □, control cells.

with 2 nM ^{125}I-α-ScTx, either in the presence of TTX, that blocks the sodium influx through the α-ScTx–activated channel, or in its absence, for 20 or 60 min. After a conventional EM procedure, morphology of cultured neurons is illustrated in Fig. 1. The different structures represented on the micrograph were classified into five compartments according to the criteria listed in Table I and were analyzed by superimposition of an array of circles (see Materials and Methods). The structures classified into the tubulovesicular compartment are illustrated in Fig. 2. The distribution of radioactivity in cellular compartments was then analyzed by centering the circles on each grain. Radioactivity was not randomly distributed, as demonstrated by a comparison of grain and circle distributions (chi-square test > 4,700, $P < 0.0001$ for all experimental conditions). After 20 or 60 min of incubations at 37°C, the crude specific radioactivity in each compartment was compared between cells exposed either with ^{125}I-α-ScTx, referred to as activated cells, or with both ^{125}I-α-ScTx and TTX i.e., control cells (Fig. 3, *A* and *B*). In the cytoplasm and the extracellular compartments, the specific radioactivity was in the same low range, although it was slightly higher in the extracellular compartment at 20 min. This difference could be due to some toxin release. The cytoplasm and the extracellular compartments did not show any significant difference in the two types of incubations. In contrast, as expected, the cell membrane was highly labeled in all the cases, resulting from the specific ^{125}I-α-ScTx binding to surface sodium channels. After a 20-min incubation (Fig. 3 *A*), the amount of ^{125}I-α-ScTx in the tubulovesicular compartment was 260% higher in activated cells compared with control cells, whereas no significant difference was observed in the cell membrane compartment. Intermediate radioactivities were found in the compartment shared between tubu-

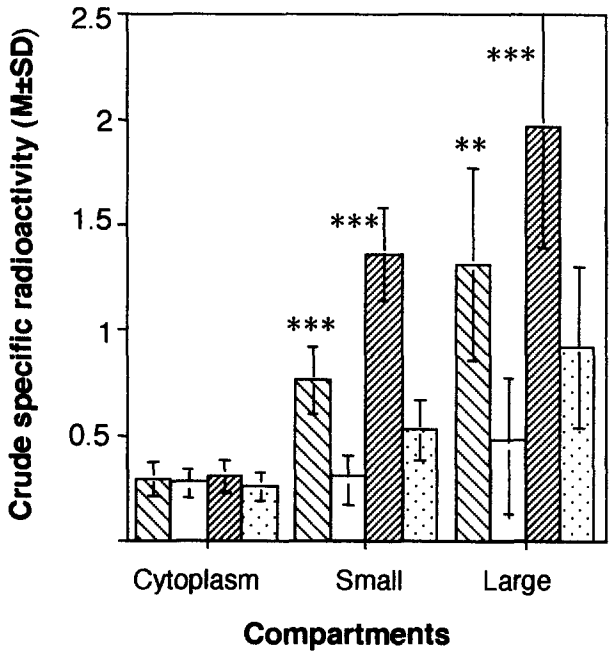

Figure 4. Distribution of the radioactivity in the tubulovesicular compartment after incubation of cultured fetal neurons with ^{125}I-α-ScTx. The definition of this compartment is given in Table I. Here, the tubulovesicular structures were divided into two separate compartments on the basis of their apparent size. Tubules or vesicles were considered large when their smallest dimension was greater than 80nm. The cytoplasmic compartment is shown for comparison. Results are expressed as mean ± SD. Asterisks indicate significant difference from activated with control cells. *t*-test: $*P < 0.05$, $**P < 0.01$, $***P < 0.001$. ▧, activated (20 min); □, control (20 min); ▨, activated (60 min); ⊡, control (60 min).

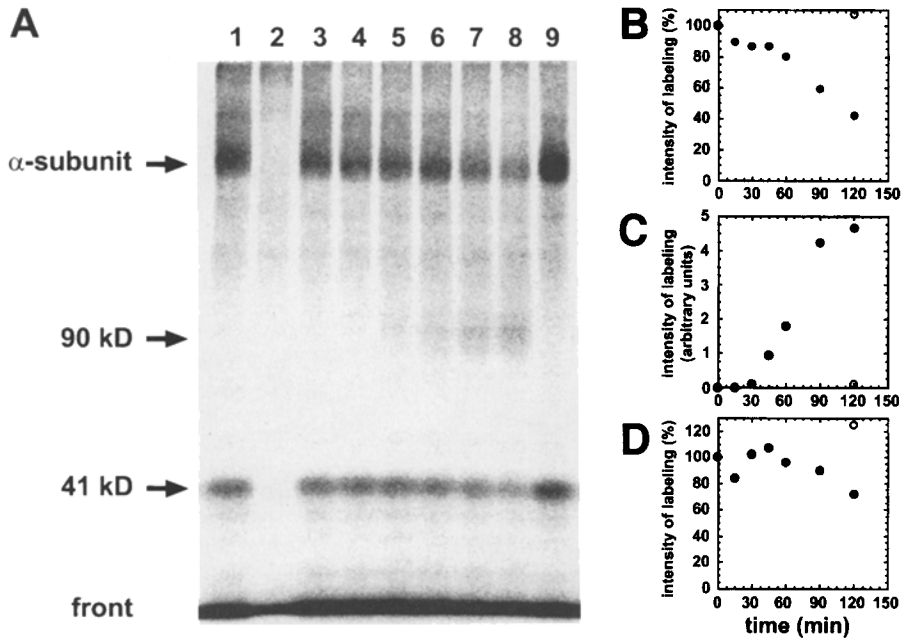

Figure 5. Veratridine activation induced a decrease in surface photolabeled sodium channels followed by degradation. (*A*) Cultured fetal neurons were photolabeled with ^{125}I-ANB-LqqV at 4°C and then exposed at 37°C to 20 μM of veratridine for various times (0, 15, 30, 45, 60, 90, and 120 min) either in the absence of TTX (1 μM) (lane *1–8*) or in its presence (lane *9*; 120 min). Nonspecific labeling was determined with a 100-fold molar excess of native α-ScTx (AaHII) (lane *2*). At the end of the incubation time, cells were homogenized and analyzed by SDS-PAGE and PhosphorImager. (*B*, *C*, and *D*) Time-course of the labeling intensity. Radioactivity in lanes *1*, and *3–9* was analyzed with a PhosphorImager and quantitated using Molecular Analyst software. After subtraction of the background radioactivity, the area of peaks corresponding to the α subunit (*B*), the 90-kD band (*C*), and the 41-kD band (*D*) were determined. Results are expressed as a percentage, 100% = radioactivity at 0 min (lane *1*) for *B* and *D*, and as arbitrary units for *C*. *Closed circles*, in absence of TTX; *open circles*, in presence of TTX.

lovesicles and the cell membrane. After a 60-min incubation (Fig. 3 *B*), when compared with control cells, the radioactivity in the cell membrane compartment of activated cells was reduced to 70% while in the tubulovesicular compartment it sharply increased by ~250% and the shared compartment showed intermediate radioactivities. At 60 min, the radioactivity of the tubulovesicular compartment in control cells was higher than that of the cytoplasm. Thus, in activated cells, ^{125}I-α-ScTx labeling was found in tubulovesicular structures inside nerve cells as soon as 20 min and reached higher levels after 60 min.

For analysis of autoradiographs, circles and grains were attributed to two size classes of tubules and vesicles. For practical purposes, the limit between "large" and "small" structures was chosen as the 1/4 of the circle diameter, that is 80 nm. The large tubulovesicular compartment included mainly large vesicles with electron-dense contents, located in soma and large cell processes. However, the small tubulovesicular compartment was composed almost exclusively of electron-lucent structures, including both small round vesicles and elongated profiles looking like tubules of the smooth endoplasmic reticulum (Fig. 2 *f*). They were located mainly in narrow processes. In grouping the initial compartments (see Material and Methods), it was possible to keep these two classes separated, despite wide errors in the large compartment values, due to the small size of this class. Comparison of cultures incubated in the presence and in the absence of TTX (Fig. 4) showed that both small and large tubulovesicular structures were significantly labeled in activated cells and the labeling increased with incubation time.

Degradation of Photolabeled Sodium Channel after Veratridine-induced Internalization

We next examined whether degradation occurs after activity-induced internalization of sodium channels by using a photoreactive α-ScTx derivative, ^{125}I-ANB-LqqV, to covalently label channels initially present at the cell surface. Cultured neurons were incubated at 37°C, in sodium medium containing 2 nM ^{125}I-ANB-LqqV. TTX (1 μM) was added during the incubation to prevent sodium channel activation induced by toxin binding. Then the cells were subjected to photolysis at 4°C for 5 min and washed at 37°C to remove noncovalently bound α-ScTx and TTX. As shown in Fig. 5 (lane *1*) and in good agreement with previous studies (Jover et al., 1988; Dargent et al., 1994), two labeled bands were detected by electrophoresis and PhosphorImager. The labeled bands have apparent molecular masses of 247 ± 13 kD and 41 kD, the large one being the sodium channel α subunit (Sharkey et al., 1984). The identity of the large component was confirmed by immunoprecipitation experiments done with antibodies directed against this subunit (data not shown). Protection from photoaffinity labeling of both bands was complete in the presence of a 100-fold excess of native α-ScTx (Fig. 5, lane *2*).

To induce an immediate and maximal activation of sodium channels after the photoaffinity labeling procedure, cultured neurons were exposed to 20 μM veratridine, which activates channels upon binding to pharmacological site 2 (Catterall, 1980). Fig. 5 (lanes *1–8*) shows that veratridine induced a decrease in the amount of both labeled bands. After 120 min, the proportion of labeled α subunits

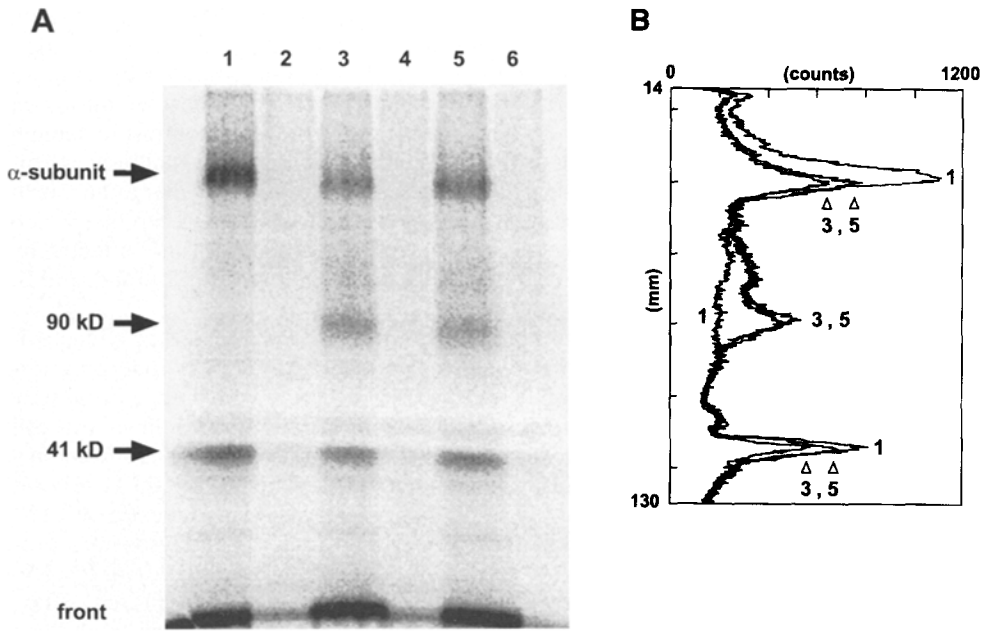

Figure 6. Amphotericin B induced a decrease in surface photolabeled sodium channels followed by degradation. (*A*) Cultured fetal neurons were photolabeled with ^{125}I-ANB-LqqV at 4°C and then exposed at 37°C to 20 μM veratridine either in presence of TTX (lanes *1* and *2*) or in its absence (lanes *3* and *4*), and to amphotericin B (5 μg/ml) (lanes *5* and *6*). After 120 min of incubation, cells were homogenized and analyzed by SDS-PAGE and the PhosphorImager. For each condition, nonspecific labeling was determined with a 100-fold molar excess of native α-ScTx (AaHII) versus the photoactivable derivative (lanes *2*, *4*, and *6*). (*B*) Radioactivity profiles corresponding to lane *1* (veratridine + TTX), lane *3* (veratridine), and lane *5* (amphotericin B).

originally at the cell surface was reduced to 40% (Fig. 5 *B*). At 45–60 min, this decrease was associated with the appearance of a major fragment of an apparent molecular mass of 90 kD (Fig. 5 *C*). After 120 min, the amount of labeled 41-kD band had decreased by 28% (Fig. 5 *D*). When TTX was added concomitantly with veratridine (lane *9*), no decrease was observed. From eight independent experiments, 120 min of veratridine treatment reduced the labeled bands by 50 ± 10% (SD) for the α subunit and 46 ± 11% (SD) for the 41 kD band, the values being normalized to control, i.e., cells incubated with veratridine and TTX. In all cases, the 90-kD band was observed. Thus, we concluded that a fraction of sodium channels initially present at the cell surface are degraded after neurotoxin-induced internalization.

Degradation of Photolabeled Sodium Channels after Amphotericin B–induced Internalization

Amphotericin B, a sodium ionophore, induced a reduction of surface sodium channels as measured by a decrease in [^{3}H]STX binding capacity and an increase in internalized ^{125}I-α-ScTx (Dargent et al., 1994). Therefore, we next examined the effect of amphotericin B on photolabeled cells (Fig. 6). As compared with control, cells incubated with veratridine and TTX (lane *1*), labeling of the α subunit was reduced to 42 and 56% in veratridine- and amphotericin B–treated cells, respectively (lanes *3* and *5*), while the labeling of the 41-kD band represented 67 and 83%. Again, the decrease in α subunit labeling (Fig. 6 *B*) was associated with the appearance of smaller molecular mass fragments with the major band of 90 kD in both cases. The effect of amphotericin B was not prevented by TTX. From two independent experiments, the remaining fraction of labeled bands was 60 ± 9% (α subunit) and 64 ± 8% (41-kD band) after 120 min of amphotericin B and TTX exposure, the values being normalized to control, i.e., cells incubated with TTX. Finally, we compared the effect of amphotericin B when the photolabeled cells were incubated either in a Na^+-containing medium (140 mM NaCl) or in a Na^+-free medium (external NaCl was replaced by 140 mM CholineCl). As shown in Fig. 7, the intensity of labeling of the α subunit and of the 41-kD band was reduced in presence of external Na^+ as compared with what observed in Na^+-free medium. Moreover, the 90-kD proteolytic fragment was only observed in the presence of external Na^+. These observations show that the effect of amphotericin B is Na^+-dependent.

Effect of Leupeptin on the Degradation of Photolabeled Sodium Channel

The photoaffinity procedure provides a specific assay for the degradation process that follows internalization. We next examined the effect of leupeptin, an inhibitor of the lysosomal proteases (Green et al., 1994). When cultured neurons were preincubated with 20 μM leupeptin, veratridine-induced down-regulation of surface sodium channels was not affected. A 36 and 42.5% decrease in the binding capacity of [^{3}H]STX, was measured in untreated cells and in leupeptin-treated cells, respectively, after 120 min of veratridine incubation. However, in photolabeled cells, the degradation of the α subunit, and the appearance of the 90-kD fragment were prevented by leupeptin (Fig. 8; Table II) whereas the decrease in the amount of 41-kD protein was unaffected. Similar results were observed when veratridine was replaced by amphotericin B (Fig. 9), while no difference was found in the amphotericin B–induced decrease in [^{3}H]STX binding capacity (39 and 40% for untreated and leupeptin treated cells, respectively). These results indicate that internalized sodium channel α subunits are delivered to the lysosomal compartment.

Discussion

The present study demonstrates that in response to sodium channel activation, cultured neurons down-regulate surface channels by a Na^+-dependent endocytotic process

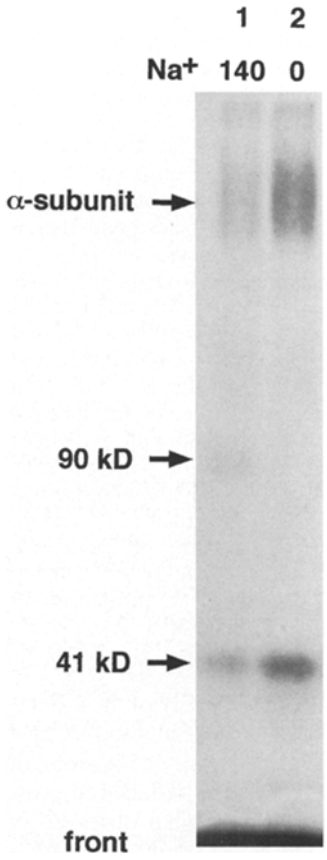

Figure 7. The effect of amphotericin B is Na^+ dependent. (*A*) Cultured fetal neurons were photolabeled with ^{125}I-ANB-LqqV at 4°C and then exposed to amphotericin B (5 μg/ml) either in a sodium medium (lane *1*) or in a sodium-free medium (lane *2*) at 37°C. After 120 min of incubation, cells were homogenized and analyzed by SDS-PAGE and autoradiography.

and deliver them to a compartment where degradation occurs. Two distinct approaches were used. First, the distribution of ^{125}I-α-ScTx, a sodium channel marker and activator, was analyzed in different subcellular compartments by quantitative EM autoradiography. Second, a photolabeling procedure was applied to monitor surface channels after their activation.

Quantitative EM autoradiography showed that, after binding to surface sodium channels, ^{125}I-α-ScTx was found to disappear from the cell surface and accumulate in tubulovesicular endosomes in a time-dependent manner. Toxin internalization was related to channel activity since it was blocked by TTX. Consistent with a previous study (Parton et al., 1992) on the endocytotic pathway in cultured hippocampal neurons, the endosomes examined in this study appeared as an extremely dense network of tubules and vesicles. The tubulovesicular endosomes were located in all processes, indicating that the cultured neurons used in the present study are less mature than polarized hippocampal neurons (Parton et al., 1992). When the endosomes were classified according to size, the large structures were located predominantly in cell bodies and in major processes, whereas the small endosomes were found in minor processes.

The possibility that the activity-induced endocytosis of sodium channels results from a general stimulation of endocytosis by Na^+ influx cannot be excluded. However, several pieces of evidence argue against this hypothesis. First, no major increase in the amount of endosomes was detected upon sodium channel activation. Second, the surface density of other membrane proteins, i.e., apamin-sensitive potassium channels, N-type calcium channels and insulin receptors was not affected by sodium channel activation (Dargent and Couraud, 1990). Since the density of these membrane proteins remains roughly constant during in vitro maturation of cultured neurons, in contrast to sodium channels, one could make the assumption that induced endocytosis only concerns newly inserted membrane proteins. However, the density of $GABA_A$ receptors, which increases during neuronal maturation, was not affected by sodium channel activation (Paillart, C., F. Couraud, and B. Dargent, unpublished results).

Photoaffinity labeling of sodium channels provided evidence that they are degraded after activity-induced internalization. This approach offers the advantage of directly monitoring sodium channels initially present at the cell surface. Activation of surface channels by veratridine resulted in a time-dependent degradation of the α subunit (the 260-kD component) that was totally blocked by TTX. Leupeptin is a well-known inhibitor of lysosomal proteases, for example, it prevents the degradation of P-selectin in lysosomes (Green et al., 1994). In the present study, sodium channel α subunit was protected from breakdown by leupeptin, while internalization still occurred. Thus, the results reported here clearly show that in response to activation, sodium channels are delivered to endosomes and then transported to a compartment where degradation occurs. These findings are in good agreement with a previous study indicating that down-regulation of surface sodium channels was irreversible (Dargent et al., 1995). Thus, during the acquisition of neuronal excitability, this regulatory mechanism might allow a neuron to adjust the number of sodium channels to an optimum density for generating action potentials. Precise control would be the result of a balance between activation-induced channel degradation and insertion of newly synthesized channel proteins.

The smaller protein specifically labeled by the α-ScTx toxin derivative had an apparent molecular mass of 34 kD after subtraction of the molecular mass of the toxin (7 kD). Early studies suggested that in cultured fetal neurons, the 34-kD band could be the sodium channel β_1 subunit (Jover et al., 1988). Recent evidence does not support this hypothesis. First, McHugh Sutkowski and Catterall (1990) have shown by Western blotting that the β_1 subunit appears as a 26-kD polypeptide during embryonic stages as well as in cultured fetal neurons, while the adult form has an apparent molecular mass of 36 kD. Second, only barely detectable amounts of β_1 transcripts were detected by Northern blotting in cultured neurons, as compared with adult rat brain (Alcaraz, G., B. Sampo, N. Tricaud, P. Giraud, M.-F. Eauclaire-Martin, F. Couraud, and B. Dargent, manuscript submitted for publication). Thus, the identity of the labeled 34-kD protein that is closely associated with the α subunit because of its specific covalent labeling with α-ScTx toxin still remains to be elucidated in cultured fetal neurons. However, the results reported here clearly show that the photolabeled 34-kD protein is internalized and degraded. In contrast to the sodium channel α subunit, this protein was not protected from degradation by leupeptin. It is possible that proteolytic cleavage that is not blocked by leupeptin occurs at a step during transport from early to late endosomes.

With regard to classical receptor-mediated endocytosis

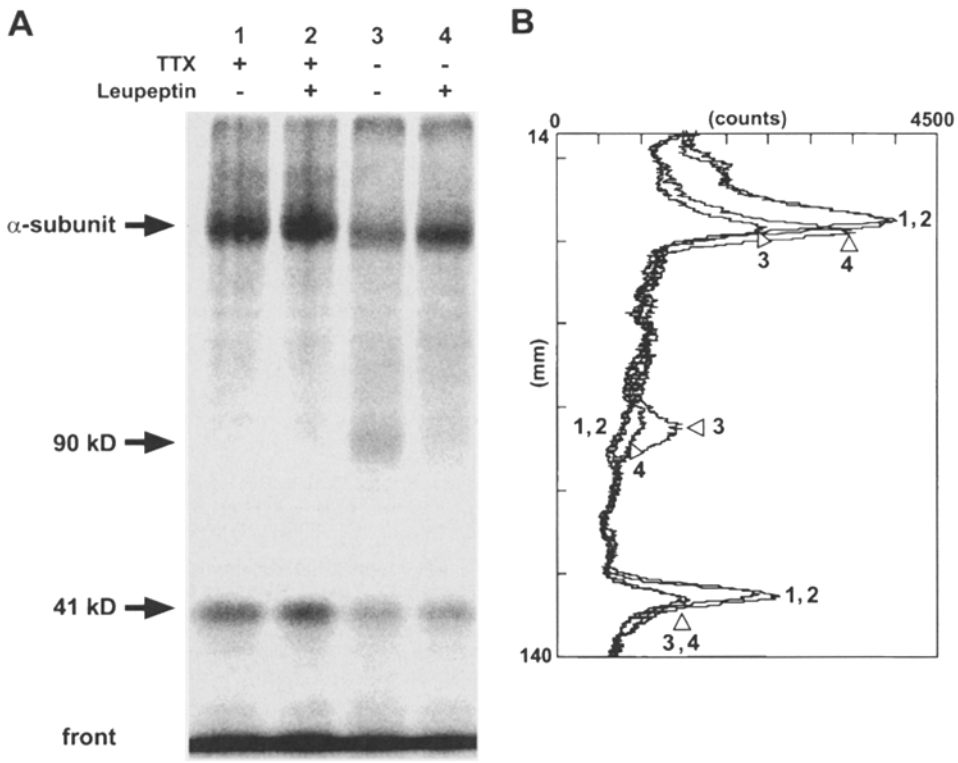

Figure 8. Effect of leupeptin on veratridine-induced degradation of sodium channels. (*A*) Photolabeled cells were preincubated at 37°C for 30 min either in the absence of leupeptin (lanes *1* and *3*) or in its presence (20 μM) (lanes *2* and *4*). Then, the cells were incubated with 20 μM veratridine either in the presence of TTX (lanes *1* and *2*) or in its absence (lanes *3* and *4*). After 120 min at 37°C, the cells were homogenized and analyzed by SDS-PAGE and the PhosphorImager. (*B*) Profiles of radioactivity corresponding to lanes *1–4*.

(Trowbridge, 1991), internalization of sodium channels is not triggered by ligand binding, but is mediated by an increase in sodium influx through the neurotoxin-activated channel. Since amphotericin B, a sodium ionophore, also causes channel internalization and degradation, an increase in intracellular Na^+ concentration ($[Na^+]_i$) triggers sodium channel endocytosis. Spontaneous activation of Na^+ channels organized in clusters might result in a significant local increase in $[Na^+]_i$ sufficient to induce internalization. Furthermore, the particular morphology of neuritic processes might favor this increase because of their high surface-to-volume ratio. It would be particularly interesting to determine the minimum increase in $[Na^+]_i$ (Kiedrowsky et al., 1994) necessary to trigger internalization. Evidence for a role of Na^+ ions in neuronal signaling is sparse. $[Na^+]_i$ regulates Ca^{++}-independent neuropeptide secretion in isolated nerve endings from the rat neurohypophysis (Nordmann and Stuenkel, 1991). The induction of cerebellar long-term depression in culture was found to require the postsynaptic action of Na^+ ions (Linden et al., 1993). In both cases, the mechanism by which $[Na^+]_i$ acts is still unknown.

Table II. Effect of Leupeptin on the Degradation of Sodium Channels

	Intensity of labeling +leupeptin/−leupeptin
Sodium channel α subunit	171 ± 24%
90-kD degradation band	20.8 ± 3%
41-kD band	105 ± 8%

Photolabeled cells were preincubated at 37°C for 30 min either in the absence of leupeptin or in its presence (20 μM). Then, the cells were incubated with 20 μM veratridine for 120 min at 37°C. After SDS-PAGE, the intensity of labeling was analyzed using the PhosphorImager in each condition. Results ± SD from three independent experiments are expressed as percentage, 100% = radioactivity in absence of leupeptin.

Another example underlines the role of $[Na^+]_i$ as a primary signal for regulating cell surface levels of integral membrane proteins. Exposure of cultured chick skeletal muscle to veratridine for 24 h, resulted in a 60–100% increase in the density of Na^+-K^+ ATPase in the plasma membrane (Wolitzky and Fambrough, 1986). Na^+-K^+ ATPase up-regulation induced by veratridine was reversed by TTX. Again, as we observed in cultured neurons (Dargent et al., 1995), neither membrane depolarization, nor elevated cytosolic Ca^{++} mediated the effect of veratridine in chick skeletal muscle. In both cell types, the transduction mechanism mediated by an increase in $[Na^+]_i$ is still unknown. It is possible that Na^+ ions that permeate through the sodium channel activate an uncharacterized protein kinase as described for nicotinic acetycholine receptors (Miles et al., 1994). In addition to regulating protein density, $[Na^+]_i$ also acts as a modulator of gene expression. Sustained activation of sodium channels results in a decrease in expression of mRNAs encoding three sodium channel α subunits in cultured neurons (Lara et al., 1996) and up-regulates the transcripts of the Na^+-K^+ ATPase β subunit in cultured myotubes (Fambrough, 1988).

During neuronal development, a Na^+-dependent endocytotic process allows a neuron to precisely regulate sodium channel density at the cell surface. This regulatory mechanism could be involved in the control of neuronal excitability. The next task will be to develop a suitable model system to elucidate the sorting determinant within the channel involved in its delivery to endosomes and to lysosomes.

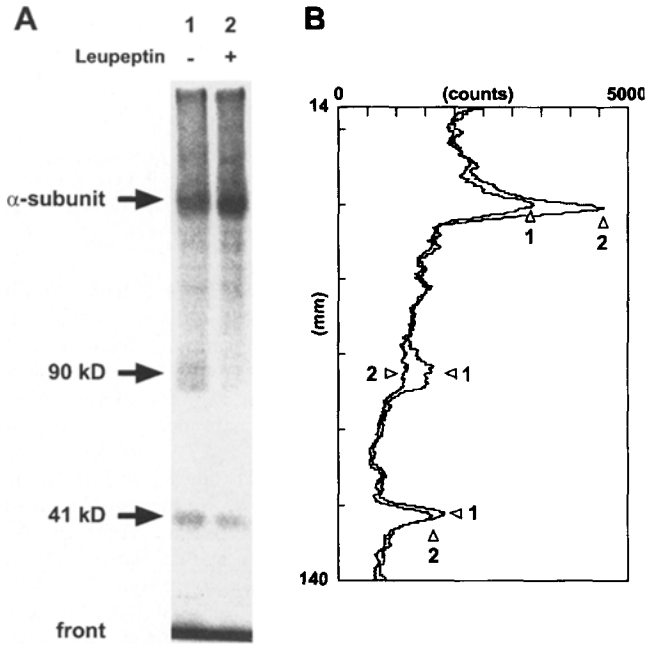

Figure 9. Effect of leupeptin on amphotericin B–induced degradation of sodium channels. (*A*) Photolabeled cells were preincubated at 37°C for 30 min either in the absence of leupeptin (lane *1*) or in its presence (20 μM) (lane *2*). Then amphotericin B (5 μg/ml) was added in the incubation medium. All incubations contained TTX. After 120 min of incubation, the cells were homogenized and analyzed by SDS-PAGE and PhosphorImager. (*B*) Profiles of radioactivity corresponding to lanes *1* and *2*.

We thank M. Seagar, G. Alcaraz, and A. J. Zamora for critical reading of the manuscript, M.-F. Martin-Eauclaire for the generous gift of α-ScTx, and F. Jullien for excellent preparation of the cell cultures.

Received for publication 25 January 1996 and in revised form 5 April 1996.

References

Beckh, S., M. Noda, H. Lübbert, and S. Numa. 1989. Differential regulation of three sodium channel messenger RNAs in the rat central nervous system during development. *EMBO (Eur. Mol. Biol. Organ.) J.* 8:3611–3616.

Boudier, J.A., Y. Berwald-Netter, H.D. Dellman, J.L. Boudier, F. Couraud, A. Koulakoff, and P. Cau. 1985. Ultrastructural visualization of Na^+ channel associated ^{125}I-α-scorpion toxin binding sites on fetal mouse nerve cells in culture. *Dev. Brain Res.* 20:137–142.

Boudier, J.L., T. Le Treut, and E. Jover. 1992. Autoradiographic localization of voltage-dependent sodium channels on the mouse neuromuscular junction using ^{125}I-α scorpion toxin. II. Sodium channel distribution on postsynaptic membranes. *J. Neurosci.* 12:454–466.

Brysch, W., O.D. Creutzfeldt, K. Lüno, R. Schlingensiepen, and K.H. Schlingensiepen. 1991. Regional and temporal expression of sodium channel messenger RNAs in the rat brain during development. *Exp. Brain Res.* 86:562–567.

Catterall, W.A. 1980. Neurotoxins that act on voltage-sensitive sodium channels in excitable membranes. *Annu. Rev. Pharmacol. Toxicol.* 20:15–43.

Dargent, B., and F. Couraud. 1990. Down-regulation of voltage-dependent sodium channels initiated by sodium influx in developing neurons. *Proc. Natl. Acad. Sci. USA.* 87:5907–5911.

Dargent, B., C. Paillart, E. Carlier, G. Alcaraz, M.F. Martin-Eauclaire, and F. Couraud. 1994. Sodium channel internalization in developing neurons. *Neuron.* 13:683–690.

Dargent, B., F. Jullien, and F. Couraud. 1995. Internalization of voltage-dependent sodium channels in fetal rat brain neurons: a study of the regulation of endocytosis. *J. Neurochem.* 65:407–413.

De Lima, M.E., F. Couraud, B. Lapied, M. Pelhate, C.R. Diniz, and H. Rochat. 1988. Photoaffinity labeling of scorpion toxin receptors associated with insect synaptosomal Na^+ channels. *Biochem. Biophys. Res. Commun.* 151: 187–192.

Fambrough, D.M. 1988. The sodium pump becomes a family. *TINS (Trends Neurosci.).* 11:325–328.

Gautron, S., G. Dos Santos, D. Pinto-Henrique, A. Koulakoff, F. Gros, and Y. Berwald-Netter. 1992. The glial voltage gated sodium channels: cell- and tissue-specific mRNA expression. *Proc. Natl. Acad. Sci. USA.* 89:7272–7276.

Green, S.A., H. Setiadi, R.P. McEver, and R.B. Kelly. 1994. The cytoplasmic domain of P-selectin contains a sorting determinant that mediates rapid degradation in lysosomes. *J. Cell Biol.* 124:435–448.

Griffiths, G.G., Werren, P. Quinn, O. Mathieu-Costello, and H. Hoppeler. 1984. Density of newly synthesized plasma membrane proteins in intracellular membranes. I. Stereological studies. *J. Cell Biol.* 98:2133–2141.

Gruenberg, J., and F.R. Maxfield. 1995. Membrane transport in the endocytic pathway. *Curr. Opin. Cell Biol.* 7:552–563.

Hartshorne, R.P., and W.A. Catterall. 1984. The sodium channel from rat brain: purification and subunit composition. *J. Biol. Chem.* 259:1667–1675.

Isom, L.L., K.S. De Jongh, D.E. Patton, B.F.X. Reber, J. Offord, H. Charbonneau, K. Walsh, A.L. Goldin, and W.A. Catterall. 1992. Primary structure and functional expression of the β_1 subunit of the rat brain sodium channel. *Science (Wash. DC).* 256:839–842.

Isom, L.L., K.S. De Jongh, and W.A. Catterall. 1994. Auxiliary subunits of voltage-gated ion channels. *Neuron.* 12:1183–1194.

Isom, L.L., T. Scheuer, A.B. Brownstein, D.S. Ragsdale, B.J. Murphy, and W.A. Catterall. 1995*a*. Functional co-expression of the β_1 and type IIA α subunits of sodium channels in a mammalian cell line. *J. Biol. Chem.* 270: 3306–3312.

Isom, L.L., D.S. Ragsdale , K.S. De Jongh, R.E. Westenbroek, B.F.X. Reber, T. Scheuer, and W.A. Catterall. 1995*b*. Structure and function of the β_2 subunit of brain sodium channels, a transmembrane glycoprotein with a CAM motif. *Cell.* 83:433–442.

Jaffe, D.B., D. Johnston, N. Lasser-Ross, J.E. Lisman, H. Miyakawa, and W.N. Ross. 1992. The spread of Na^+ spikes determines the pattern of dendritic Ca^{2+} entry into hippocampal neurons. *Nature (Lond.).* 357:244–246.

Joho, R.J., J.R. Moorman, A.M.J. VanDongen, G.E. Kirsch, H. Silberberg, G. Schuster, and A.M. Brown. 1990. Toxin and kinetic profile of rat brain type III sodium channels expressed in *Xenopus* oocytes. *Mol. Brain. Res.* 7: 105–113.

Jover, E., A. Massacrier, P. Cau, M.F. Martin, and F. Couraud. 1988. The correlation between Na^+ channel subunits and scorpion toxin binding sites. *J. Biol. Chem.* 263:1542–1548.

Kiedrowski, L., J.T. Wroblewski, and E. Costa. 1994. Intracellular sodium concentration in cultured cerebellar granule cells challenged with glutamate. *Mol. Pharmacol.* 45:1050–1054.

Lara, A., B. Dargent, F. Jullien, G. Alcaraz, N. Tricaud, F. Couraud, and E. Jover. 1996. Channel activators reduce the expression of sodium channel α-subunit mRNA in developing neurons. *Mol. Brain Res.* 37:116–124.

Larra, F., and B. Droz. 1970. Techniques radioautographiques et leur application à l'étude du renouvellement des constituants cellulaires. *J. Microscopie.* 9:845–880.

Linden, D.J., M. Smeyne, and J.A. Connor. 1993. Induction of cerebellar long term depression in culture requires postsynaptic action of sodium ions. *Neuron.* 11:1093–1100.

Magee, J.C., and D. Johnston. 1995. Synaptic activation of voltage-gated channels in the dendrites of hippocampal pyramidal neurons. *Science (Wash. DC).* 268:301–304.

Maizel, J., Jr. 1971. Polyacrylamide gel electrophoresis of viral proteins. *Methods Virol.* 5:179–224.

Makita, N., P.B. Bennett, and A.L. George. 1994. Voltage-gated Na^+ channel β_1 subunit mRNA expressed in adult human skeletal muscle, heart, and brain is encoded by a single gene. *J. Biol. Chem.* 269:7571–7578.

Mandel, G. 1992. Tissue specific expression of the voltage-sensitive sodium channel. *J. Memb. Biol.* 125:193–205.

Martin, M.-F., and H. Rochat. 1986. Large scale purification of venon of *Androctonus australis* Hector. *Toxicon.* 24:1131–1139.

McHugh Sutkowski, E., and W.A. Catterall. 1990. β_1 subunits of sodium channels. Studies with subunit-specific antibodies. *J. Biol. Chem.* 265:12393–12399.

Miles, K., S. Audigier, P. Greengard, and R.L. Huganir. 1994. Autoregulation of phosphorylation of the nicotinic acetylcholine receptor. *J. Neurosci.* 14: 3271–3279.

Noda, M., T. Ikeda, T. Kayano, H. Suzuki, H. Takeshima, M. Kurasaki, T. Takahashi, and S. Numa. 1986. Expression of functional sodium channel from cloned cDNA. *Nature (Lond.).* 322:826–828.

Nordmann, J.J., and E.L. Stuenkel. 1991. Ca^{2+}-independent regulation of neurosecretion by intracellular Na^+. *FEBS Lett.* 292:37–41.

Parton, R.G., K. Simons, and C.G. Dotti. 1992. Axonal and dendritic endocytic pathways in cultured neurons. *J. Cell Biol.* 119:123–137.

Schaller, K.L., D.M. Krzemien, P.J. Yarowsky, B.K. Krueger, and J.H. Caldwell. 1995. A novel, abundant sodium channel expressed in neurons and glia. *J. Neurosci.* 15:3231–3242.

Scheuer, T.L., V.J. Auld, S. Boyd, J.R. Offord, and W.A Catterall. 1990. Functional properties of rat brain sodium channels expressed in somatic cell line. *Science (Wash. DC).* 247:854–858.

Sharkey, R.G., D.A. Beneski, and W.A. Catterall. 1984. Differential labeling of the α and β_1 subunits of the sodium channel by photoreactive derivatives of scorpion toxin. *Biochemistry.* 23:6078–6086.

Spruston, N., Y. Schiller, G. Stuart, and B. Sakmann. 1995. Activity-dependent action potential invasion and calcium influx into hippocampal CA1 dendrites. *Science (Wash. DC).* 268:297–300.

Stuart, G.J., and B. Sakmann. 1994. Active propagation of somatic action potentials into neocortical pyramidal cell dendrites. *Nature (Lond.).* 367:69–72.

Suzuki, H., S. Beckh, H. Kubo, N. Yahagi, H. Isshida, T. Kayano, M. Noda, and S. Numa. 1988. Functional expression of cloned cDNA encoding sodium channel III. *FEBS Lett.* 1:195–200.

Trowbridge, I.S. 1991. Endocytosis and signals for internalization. *Curr. Opin. Cell Biol.* 3:634–641.

Waxman, S.G., and J.M Ritchie. 1985. Organization of ion channels in the myelinated nerve fiber. *Science (Wash. DC).* 228:1502–1507.

Westenbroek, R.E., D.K. Merrick, and W.A. Catterall. 1989. Differential subcellular localization of the RI and RII Na^+ channel subtypes in central neurons. *Neuron.* 3:695–704.

Williams, M. A. 1977. The analysis of electron microscope autoradiographs. In Quantitative Methods in Biology. (M.A. Williams, editor) North-Holland Publishing Co., Amsterdam. 85–169.

Wolitzky, B.A., and D.M. Fambrough. 1986. Regulation of the (Na^++K^+)-ATPase in cultured chick skeletal muscle. Modulation of expression by the demand for ion transport. *J. Biol. Chem.* 261:9990–9999.

Wollner, D.A., and W.A. Catterall. 1986. Localization of sodium channels in axon hillocks and initial segments of retinal ganglion cells. *Proc. Natl. Acad. Sci. USA.* 83:8424–8428.